01 Jan 2006

Electrochemical Deposition and Characterization of Fe_3O_4 Films Produced by the Reduction of Fe(III)-triethanolamine

Hiten M. Kothari

Elizabeth A. Kulp

Steven J. Limmer

Philippe Poizot

et. al. For a complete list of authors, see https://scholarsmine.mst.edu/chem_facwork/2349

Recommended Citation

H. M. Kothari et al., "Electrochemical Deposition and Characterization of Fe_3O_4 Films Produced by the Reduction of Fe(III)-triethanolamine," *Journal of Materials Research*, vol. 21, no. 1, pp. 293-301, Materials Research Society, Jan 2006.
The definitive version is available at https://doi.org/10.1557/jmr.2006.0030

Electrochemical deposition and characterization of Fe_3O_4 films produced by the reduction of Fe(III)-triethanolamine

Hiten M. Kothari, Elizabeth A. Kulp, Steven J. Limmer, Philippe Poizot, Eric W. Bohannan, and Jay A. Switzer[a)]
Department of Chemistry and Graduate Center of Materials Research, University of Missouri–Rolla, Rolla, Missouri 65409-1170

(Received 2 August 2005; accepted 21 October 2005)

In this paper, we demonstrate that films of magnetite, Fe_3O_4, can be deposited by the electrochemical reduction of a Fe(III)-triethanolamine complex in aqueous alkaline solution. The films were deposited with a columnar microstructure and a [100] preferred orientation on stainless steel substrates. In-plane electrical transport and magnetoresistance measurements were performed on the films after they were stripped off onto glass substrates. The resistance of the films was dependent on the oxygen partial pressure. We attribute the increase in resistance in O_2 and the decrease in resistance in Ar to the oxidation and reduction of grain boundaries. The decrease in resistance in an Ar atmosphere exhibited first-order kinetics, with an activation energy of 0.2 eV. The temperature dependence of the resistance showed a linear dependence of log(R) versus $T^{-1/2}$, consistent with tunneling across resistive grain boundaries. A room-temperature magnetoresistance of −6.5% was observed at a magnetic field of 9 T.

I. INTRODUCTION

Magnetite (Fe_3O_4) is a half-metallic metal oxide with the inverse spinel structure and space group *Fd*3*m*. Below the Curie temperature of 860 K, magnetite exhibits ferrimagnetism. The octahedral sites are shared by Fe^{3+} and Fe^{2+} ions, while the tetrahedral sites are occupied by Fe^{3+} ions. The moments from the Fe^{3+} ions cancel, yielding a net ferrimagnetism due to the moments on the Fe^{2+} sites. The material is a promising candidate for magnetic memory and spin-dependent transport devices because it has a calculated spin polarization of 100% at the Fermi level.[1,2] A negative spin polarization for Fe_3O_4 has also been experimentally verified by spin polarized photoemission spectroscopy[3,4] and by magnetoresistance measurements on $Fe_3O_4/CoCr_2O_4/La_{0.7}Sr_{0.3}MnO_3$ magnetic trilayer junctions.[5] Magnetoresistance devices have been produced based on Fe_3O_4 in which spin-polarized electrons are injected across thin tunnel barriers,[6] resistive grain boundaries,[7–9] antiphase boundaries,[10] and nanocontacts.[11]

Magnetite films have been deposited onto polycrystalline and single-crystal substrates using pulsed laser ablation,[12–15] molecular beam epitaxy,[16–18] and by oxidizing Fe thin films.[19,20] Our interest is in the epitaxial electrodeposition of metal oxide thin films onto single-crystal substrates.[4,21–33] We have previously electrodeposited epitaxial films of Fe_3O_4 onto single-crystal Au substrates using anodic deposition.[4,23] The method was a modification of the ferrite plating process developed by Abe and co-workers.[9,34,35] Ansermet and co-workers have recently used the anodic deposition method to produce nanocrystalline Fe_3O_4.[36] In our previous work, Fe(II) was electrochemically oxidized in an Ar atmosphere at 90 °C to Fe_3O_4. A problem with this method is that Fe(II) is also oxidized to Fe_3O_4 powder by molecular oxygen in a homogeneous reaction, so much care must be taken to exclude molecular oxygen. In the present work, we demonstrate that Fe_3O_4 films can be produced by cathodic deposition, by the electrochemical reduction of Fe(III) complexed with triethanolamine (TEA). This is a modification of a hydrothermal method developed by Sapieszko and Matijevic to produce Fe_2O_3 and Fe_3O_4 powders from Fe(III)-TEA in the presence of oxidizing or reducing agents at 250 °C.[37] In our process, the Fe(III) is reduced electrochemically to produce Fe_3O_4 films at temperatures in the 60–90 °C range. It is not necessary to exclude molecular oxygen from this cathodic deposition bath. We also report on the electrical transport and

[a)]Address all correspondence to this author.
e-mail: jswitzer@umr.edu
This author was an editor of this journal during the review and decision stage. For the *JMR* policy on review and publication of manuscripts authored by editors, please refer to http://www.mrs.org/publications/jmr/policy.html.
DOI: 10.1557/JMR.2006.0030

magnetoresistive properties of columnar Fe_3O_4 films deposited onto stainless steel substrates.

II. EXPERIMENTAL PROCEDURES

A. Deposition solution

The films of Fe_3O_4 were electrodeposited from an alkaline solution of $Fe_2(SO_4)_3$ complexed with triethanolamine (TEA). The concentrations in the deposition bath were 0.09 M Fe(III), 0.1 M TEA, and 2 M NaOH. The solution was prepared by slowly adding Fe(III) dissolved in water to a stirred solution of NaOH and TEA at 60 °C. $Fe_2(SO_4)_3$ hydrate, TEA, and NaOH were purchased from Aldrich (Milwaukee, WI). The solutions were not sensitive to oxygen from the air, but they did slowly decompose when maintained at temperatures of 80 and 90 °C.

B. Electrochemical methods

Electrochemical experiments were performed using an EG&G Princeton Applied Research model 2273 (Oak Ridge, TN) potentiostat/galvanostat. The depositions and voltammograms were conducted in an undivided cell, with the solution exposed to the atmosphere. An Ag/AgCl electrode served as the reference. The working electrode was Au with an area of 0.02 cm^2 purchased from Bioanalytical Systems (West Lafayette, IL) for the cyclic voltammetric experiments that were used to characterize the deposition process. The deposition solution was not stirred for the cyclic voltammetry experiments. The films for x-ray diffraction (XRD), scanning electron microscopy (SEM), electrical transport, and magnetoresistance studies were deposited onto a stainless steel (SS430) electrode with the geometric area controlled to 1 cm^2 by mounting the electrode in a flat specimen holder (Model K0105 purchased from Princeton Applied Research, Oak Ridge, TN). The Au and stainless steel electrodes were mechanically polished to a mirror finish and sonicated in acetone prior to use.

C. X-ray diffraction and scanning electron microscope measurements

XRD measurements were performed with a high-resolution Philips X'Pert MRD diffractometer (Eindhoven, The Netherlands). The primary optics module was a combination Göbel mirror and 2-crystal Ge(220) 2-bounce hybrid monochromator, and the secondary optics module was a 0.18° parallel plate collimator. The hybrid monochromator produces pure Cu $K_{\alpha 1}$ radiation (λ = 0.1540562 nm) with a divergence of 25 arc seconds. The morphology of the films was probed using plan-view and cross-sectional SEM. Plan-view micrographs were obtained on a JEOL T330A SEM (Peabody, MA), while the cross-sectional image was obtained on an Hitachi S4700 SEM (Pleasanton, CA). The sample for cross-sectional analysis was produced by stripping a film that had been electrodeposited at 80 °C on a stainless steel substrate onto a glass microscope slide using 3M Super Glue (St. Paul, MN). The glass slide was cleaved to produce the cross section.

D. Electrical transport and magnetoresistance measurements

Electrical transport and magnetoresistance measurements were made on the Fe_3O_4 films after they were removed from the stainless steel substrates using 3M Super Glue. The four point resistivity of the films was first measured in air using an Alessi model CPS-06 contact probe station (Irvine, CA) with Keithley model 220 programmable current source and model 181 nanovoltmeter (Cleveland, OH). The atmosphere dependence of the film resistance was measured with a home-built polycarbonate chamber that enabled the atmosphere to be switched from Ar to O_2. The measurements of the temperature and magnetic field dependence of the resistance of the Fe_3O_4 were performed in the Quantum Design Physical Property Measurement System (PPMS, San Diego, CA). Two silver wires were attached to the Fe_3O_4 film using In metal. For these measurements, the resistance was high enough that that it was not necessary to use the four-point method. The sample was then encapsulated in Celvaseal (West Chester, PA), a silicone-resin-based high vacuum leak sealant obtained from SPI supplies.

III. RESULTS AND DISCUSSION

A. Electrochemistry

Films of Fe_3O_4 were electrodeposited by reduction of the Fe(III)-TEA complex in an aqueous alkaline bath at elevated temperatures. Cyclic voltammograms (CV) on an Au working electrode were run to characterize the cathodic deposition process, and to determine the appropriate current densities or applied potentials to use for electrodeposition. Figure 1 shows CVs at a scan rate of 50 mV/s in the unstirred deposition bath at temperatures of 60, 70, and 80 °C. For the 80 °C deposition bath, the separation between the anodic and cathodic peaks is 100 mV. The reduction begins at about −1.00 V and reaches a cathodic peak at −1.13 V versus Ag/AgCl. The anodic peak is located at −1.03 V versus Ag/AgCl. If the electrode is repetitively scanned over the potential range shown in Fig. 1, or if the electrode is poised at any potential between −1.00 and −1.13 V versus Ag/AgCl, a black film of Fe_3O_4 is deposited on the electrode. A two-step electrochemical reduction and precipitation reaction is proposed. In the first step, the Fe(III)-TEA complex is electrochemically reduced to Fe^{2+} and TEA. The electrochemically produced Fe^{2+} next reacts chemically with Fe(III)-TEA in solution to produce Fe_3O_4. The proposed mechanism is outlined in Eqs. (1) and (2):

$$\mathrm{Fe(TEA)}^{3+} + e^- \rightarrow \mathrm{Fe}^{2+} + \mathrm{TEA} \quad , \qquad (1)$$

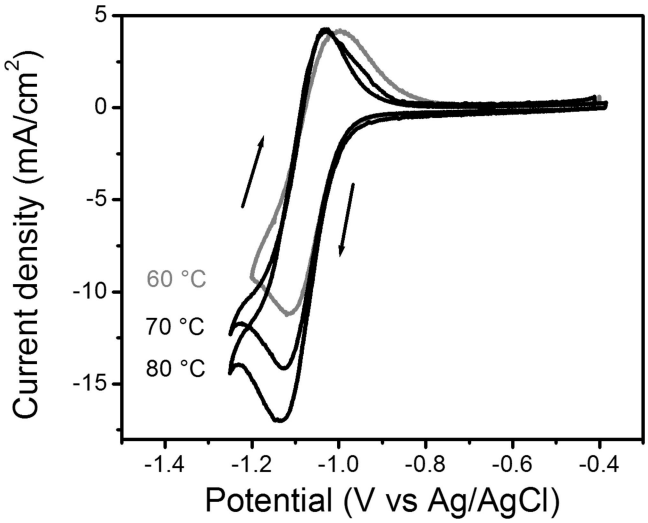

FIG. 1. Cyclic voltammograms in the Fe_3O_4 deposition solution at temperatures of 60, 70, and 80 °C. The voltammograms were run on a 0.02 cm^2 Au electrode in an unstirred solution at a scan rate of 50 mV/s.

$$Fe^{2+} + 2Fe(TEA)^{3+} + 8OH^- \rightarrow Fe_3O_4 + 2TEA + 4H_2O \quad . \tag{2}$$

Although the CVs in Fig. 1 appear to be quasireversible, our experiments indicate that the process is more complicated than the CVs suggest. For example, the cathodic peaks increase in intensity as the temperature of the solution is increased, consistent with the increase in diffusivity of the $Fe(TEA)^{3+}$ as the temperature is increased. However, the anodic peak intensity is nearly the same at all of the temperatures. Also, as shown in Fig. 2, the anodic peak current increases linearly as the applied scan rate in increased, consistent with the oxidation of a surface species. If the anodic peak were due to the diffusion-limited oxidation of unreacted Fe^{2+} in solution, then the current should increase linearly with the square root of the scan rate. Based on these observations, we believe that the anodic peaks in Fig. 1 are due to the oxidation of surface Fe_3O_4 to Fe_2O_3, according to Eq. (3). If this interpretation of the CVs is correct, it should be possible in future work to deposit Fe_3O_4/Fe_2O_3 superlattices by simple pulsing or cycling the potential during film growth.

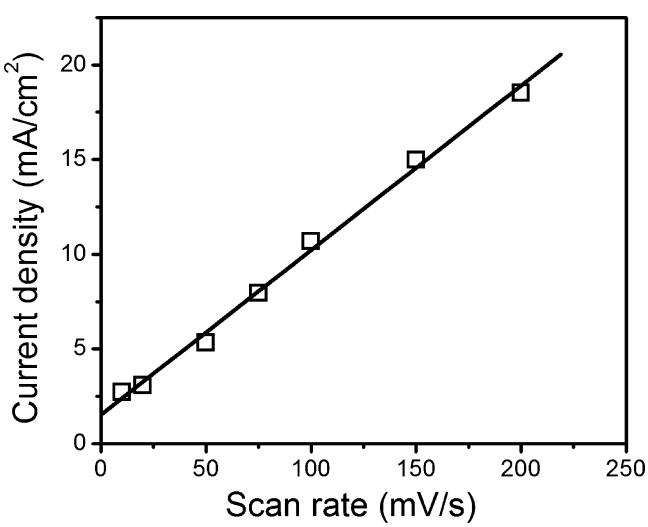

FIG. 2. Scan rate dependence of the anodic peak intensity for the cyclic voltammogram of the Au electrode in the deposition solution at 70 °C. The linear dependence indicates that the oxidation reaction occurs on the electrode surface, and is not limited by diffusion of solution species.

$$2Fe_3O_4 + 2OH^- \rightarrow 3Fe_2O_3 + H_2O + 2e^- \quad . \tag{3}$$

The films for structural, electrical, and magnetoresistance studies were electrodeposited on 15 mm diameter stainless steel samples (SS430) mounted in a flat specimen holder (Model K0105) purchased from Princeton Applied Research. The exposed area was 1 cm^2. The films were deposited at a fixed current density of 2 mA/cm^2 for 500 s at temperatures ranging from 60 to 90 °C. For a film deposited at 80 °C, the electrode potential was 1.01 V versus Ag/AgCl during the constant current deposition. The charge density passed after 500 s was 1 C/cm^2, producing a film of Fe_3O_4 that was 3 μm thick (measured with the Dektak IIA surface profiler, Santa Barbara, CA). The current efficiency for film deposition at 80 °C was approximately 65%, assuming one electron transferred in the reduction reaction and a film density equal to the crystallographic density.

B. XRD and SEM characterization of the films

Figure 3 shows θ-2θ x-ray diffraction scans of Fe_3O_4 films deposited on the SS430 substrates at temperatures of (a) 60 °C, (b) 70 °C, (c) 80 °C, and (d) 90 °C. The films were all deposited at a constant current density of 2 mA/cm^2 to a charge density of 1 C/cm^2. The films are all crystalline, and only have peaks corresponding to Fe_3O_4. The lattice parameters (shown in Table I) are all slightly larger than the lattice parameter of 0.8396 nm (space group = $Fd3m$) reported in JCPDS #19-0629 for Fe_3O_4. The material can be differentiated from maghemite (a = 0.83515 nm, JCPDS #39-1346) because the mixed-index reflections such as (110), (210), (211) of maghemite (space group = $P4_132$) are systematically absent in the electrodeposited film. The lattice parameter for the film deposited at 60 °C is 0.8401 nm, and the remaining films have lattice parameters which average about 0.843 nm. Although the peak positions correlate fairly well with those of the standard powder pattern, the peak intensities indicate that all of the films have a [100] preferred orientation. Table I shows the ratio of the intensities of the (400) and the (311) reflections ($I_{(400)}/I_{(311)}$). The $I_{(400)}/I_{(311)}$ ratio is 0.20 in the standard powder pattern, but it varies from 0.55 to 1.38 for the electrodeposited films. The strongest [100] texture is

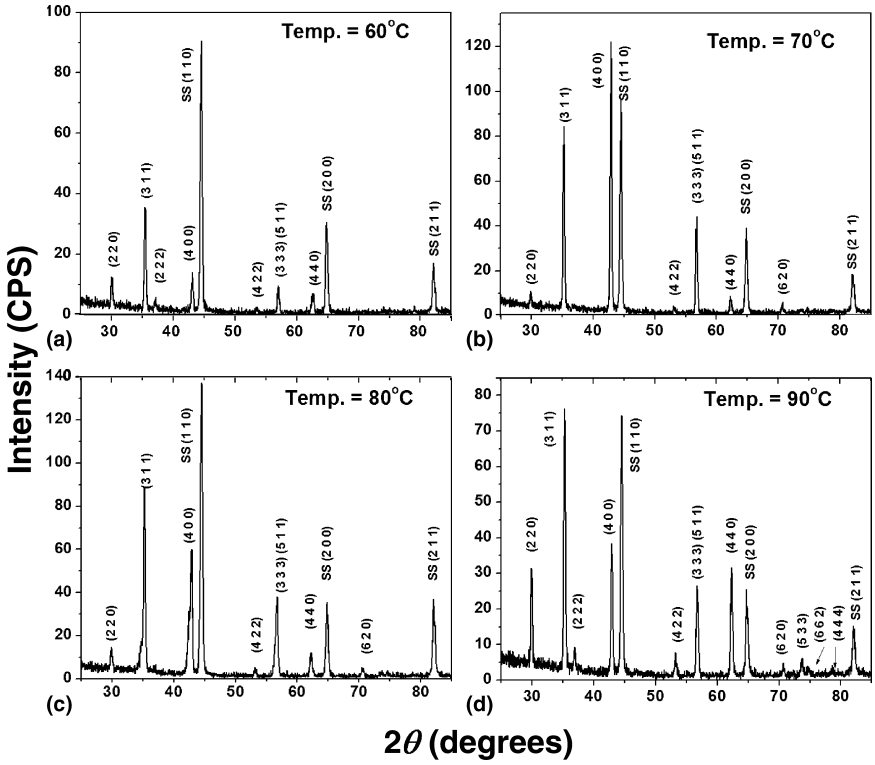

FIG. 3. X-ray diffraction scans of Fe_3O_4 films deposited on stainless steel at (a) 60 °C, (b) 70 °C, (c) 80 °C, and (d) 90 °C. The films were deposited at a constant current density of 2 mA/cm^2 to a thickness of approximately 3 μm.

TABLE I. Lattice parameters and ratios of the intensities of the (400) and (311) peaks from XRD for Fe_3O_4 as a function of deposition temperature.

Deposition temperature (°C)	Lattice parameter (nm)	$I_{(400)}/I_{(311)}$ from XRD
60	0.8401	0.60
70	0.8435	1.38
80	0.8429	0.83
90	0.8434	0.55

observed for the film deposited at 70 °C, with $I_{(400)}/I_{(311)} = 1.38$.

The crystalline nature of the films is also confirmed by the plan-view SEM images in Fig. 4 for films deposited at (a) 60 °C, (b) 70 °C, (c) 80 °C, and (d) 90 °C at a constant current density of 2 mA/cm^2 to a charge density of 1 C/cm^2. The degree of faceting of the films increases as the temperature is increased. The films deposited at 60 °C have a globular morphology, with no well-defined crystal morphology. The grain size increases as the temperature of the deposition bath is increased from 70 to 90 °C. The films deposited at 70 and 80 °C, have a pyramidal microstructure consistent with the [100] preferred orientation observed by XRD. The film deposited at 90 °C has a different morphology, suggesting that the film may be undergoing a change of orientation. Another indication that the film may undergo a change of orientation at 90 °C is the fact that the relative intensity of the (220) and (440) reflections in the XRD pattern are higher in this sample [see Fig. 3(d)] than they are in the films deposited at lower temperatures.

The films deposit with a columnar microstructure. A sample was prepared for cross-sectional SEM characterization by depositing a Fe_3O_4 film at 80 °C at a constant current density of 2 mA/cm^2 to a charge density of 1 C/cm^2. The film was then stripped off of the substrate onto a glass microscope slide using super glue. The cross-sectional sample was then prepared by cleaving the glass slide. The cross-sectional SEM view of the film is shown in Fig. 5. The film grows with a columnar morphology. The Fe_3O_4 columns are approximately 3 μm long and 0.5 μm in diameter.

C. Electrical transport and magnetoresistance of the films

Because the films are electrodeposited onto conducting stainless-steel substrates, care must be taken to ensure that the electrical properties of the film, and not the substrate, are probed. Since the sheet resistance of the electrodeposited Fe_3O_4 is considerably larger than that of the substrate, a significant fraction of the applied current in a four-point measurement will pass through the substrate instead of the sample, yielding a measured resistivity which is smaller than the actual film resistivity. To obviate this problem, the films were stripped off onto

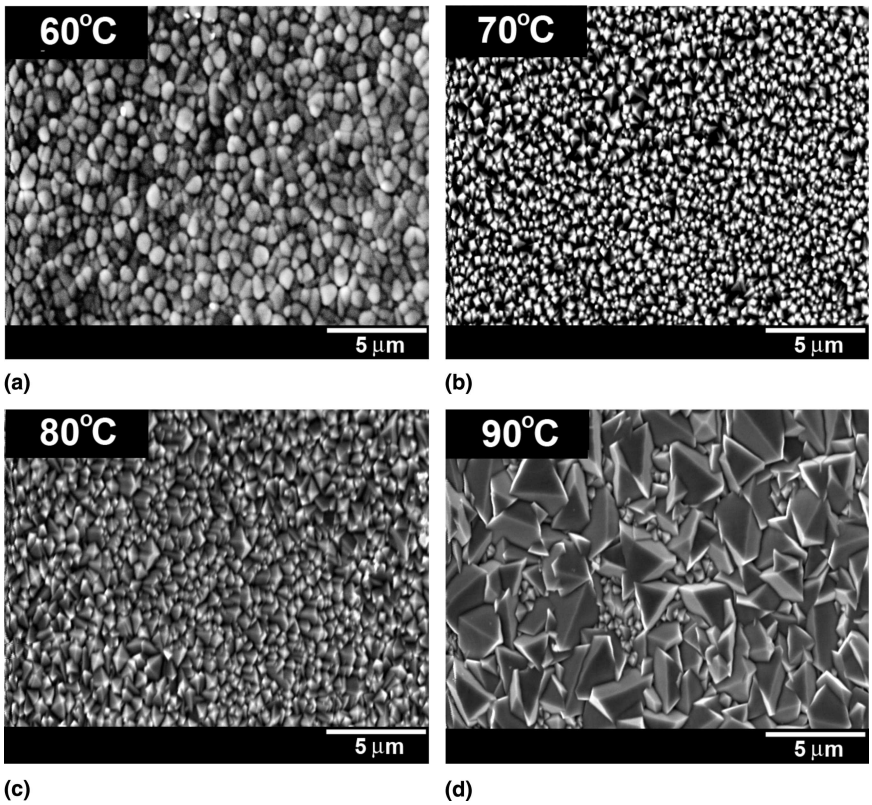

FIG. 4. Plan-view SEM images of Fe_3O_4 films deposited on stainless steel at (a) 60 °C, (b) 70 °C, (c) 80 °C, and (d) 90 °C. The films were deposited at a constant current density of 2 mA/cm^2 to a thickness of approximately 3 μm.

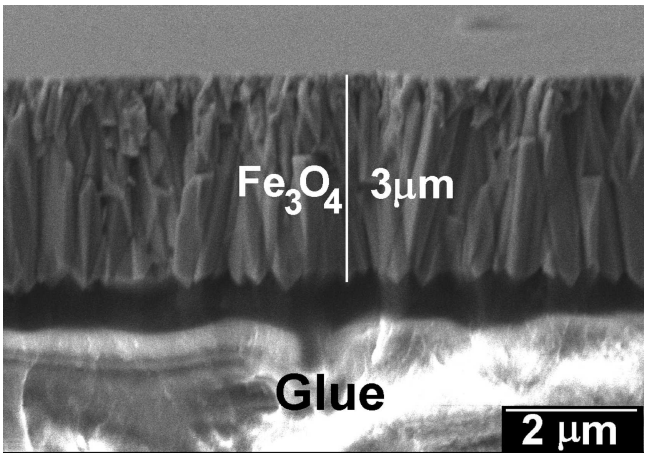

FIG. 5. Cross-sectional SEM image of a columnar Fe_3O_4 film deposited on stainless steel at 80 °C at a fixed current density of 2 mA/cm^2.
.

glass microscope slides, as described in the previous section for the production of SEM cross sections. The four-point resistivity of a 3-μm film of material that was electrodeposited at 80 °C was 0.1 Ω cm. This resistivity is about an order of magnitude higher than that reported for single-crystal and epitaxial Fe_3O_4.[7] We attribute this higher resistivity to resistive grain boundaries in the columnar Fe_3O_4 films.

Another indication that the grain boundaries may be controlling electrical transport through the samples is that the resistivity of the films is a function of the atmosphere to which the electrodeposited films are exposed. We observed that samples inserted into the He atmosphere of the Quantum Design PPMS instrument for magnetoresistance measurents showed a decrease in resistance compared with that observed for samples exposed to air. To test this atmosphere dependence of the film resistance, a sample chamber was constructed in which the resistance of the film was measured when the atmosphere was switched from pure O_2 to pure Ar. Figure 6(a) shows the effect of Ar and O_2 atmospheres on the in-plane resistance of a Fe_3O_4 film at room temperature. The resistance decreases in Ar and increases in O_2. The kinetics of the decrease in resistance was monitored in the Quantum Design PPMS sample chamber maintained under a He atmosphere. The samples were first equilibrated in air before inserting in the He atmosphere. Figure 6(b) shows the first-order decay fit for the drop in resistance of a Fe_3O_4 film at 300 K. The first order rate constant k for the decay is 0.0069 min^{-1}, corresponding to a half life of 100 min. The resistance change is kinetically limited, as opposed to a diffusion limited reaction, which would have resulted in a $t^{-1/2}$ dependence. We also determined the temperature dependence of the first order rate constants for film reduction. The activation energy

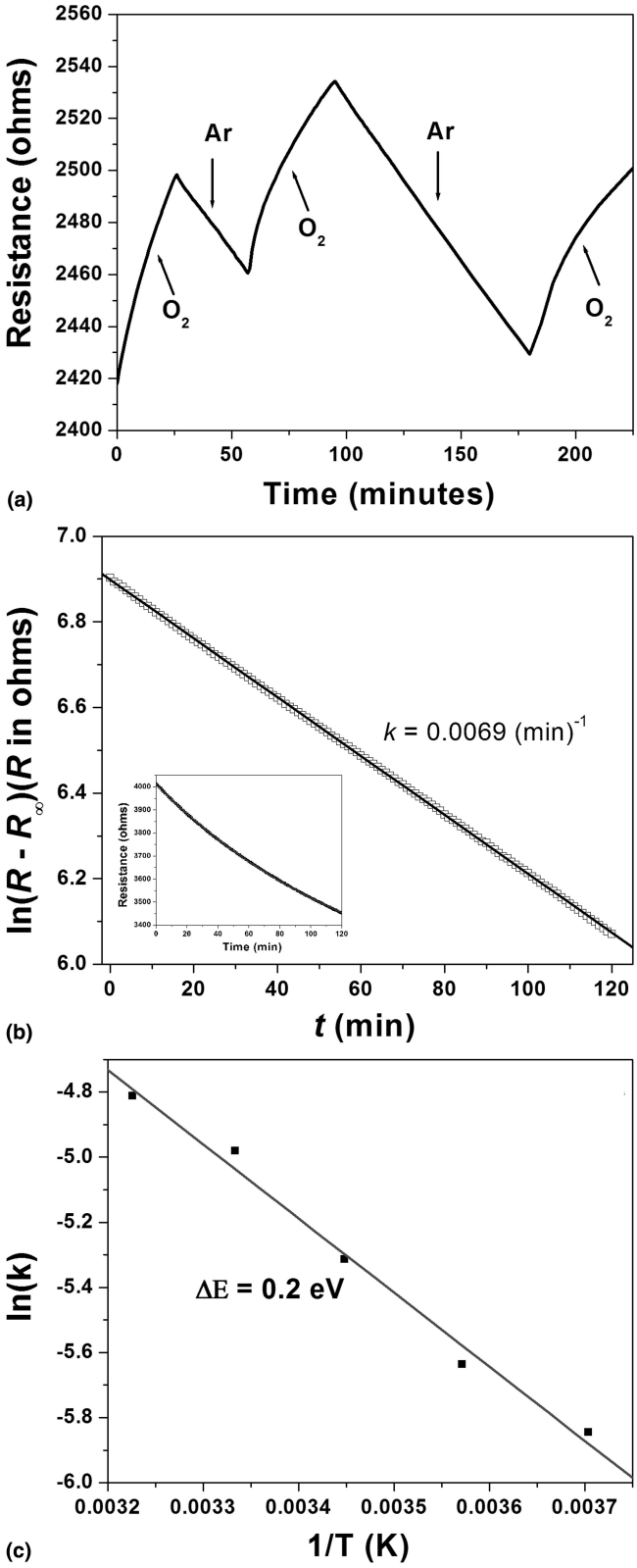

FIG. 6. Atmosphere dependence of the in-plane resistance of the electrodeposited Fe_3O_4. (a) Effect of O_2 and Ar atmospheres on the in-plane resistance. (b) First-order decay for the drop in resistance in a He atmosphere at 300 K. (c) Determination of the activation energy for film reduction from a plot of ln(k) versus $1/T$.

derived from the slope of the Arrhenius plot of ln(k) versus $1/T$ in Fig. 6(c) is 0.2 eV.

We attribute the increase in in-plane resistance of the Fe_3O_4 films when they are transferred from an inert atmosphere to an O_2 atmosphere to the oxidation of the films to γ–Fe_2O_3 at the columnar grain boundaries. The decrease in resistance in an Ar atmosphere suggests that the grain boundaries are reducing back to Fe_3O_4 in the Ar atmosphere. The oxidation of Fe_3O_4 to γ–Fe_2O_3 at room temperature in the presence of O_2 has been reported for thin films of Fe_3O_4 grown on MgO substrates.[38,39] Saunders and Gallagher have reported the oxidation of Fe_3O_4 to α–Fe_2O_3 via a metastable γ–Fe_2O_3 using a thermomagnetometric study.[40] Oxidation of dry Fe_3O_4 powders has been reported to be limited by the outward diffusion of Fe^{2+} ions.[41,42] Recently, a diffusion limited oxidation of Fe_3O_4 nanoparticles to γ–Fe_2O_3 in solution has been monitored using optical spectroscopy.[43] The activation energy for the oxidation of Fe_3O_4 nanoparticles was 0.91 eV,[43] compared with the value of 0.2 eV that we measured for the reverse reaction. It is difficult to compare these activation energies because the oxidation reaction is a bulk diffusion-limited process, and the reduction reaction is a kinetically-controlled grain boundary reaction. We believe that the ability to control the grain boundary resistance of electrodeposited Fe_3O_4 films will become important when optimizing the performance of spin-dependent transport devices based on Fe_3O_4. The grain boundary resistance can be tuned by subjecting the film to an atmosphere with the appropriate oxygen partial pressure, and then that resistance can be "locked-in" by encapsulating the sample.

For our electrical transport and magnetoresistance studies the samples were coated with Celvaseal, a silicone resin from SPI supplies that is used as a high vacuum sealant. A schematic illustration of the sample configuration for these measurements is shown in Fig. 7. Prior to coating with Celvaseal, two point contacts were made to the sample using Ag wires attached to the sample with In metal. The coating process eliminated the atmosphere dependence observed with the uncoated samples. The in-plane resistance was monitored as a function of temperature. As shown in Fig. 8, a linear fit is observed for a plot of $\log(R)$ versus $T^{-1/2}$. This fit is consistent with the model of tunneling across grain boundaries developed by Sheng et al. for electrical transport in composites made of metal particles in an insulating matrix.[44] Liu et al. have reported the same temperature dependence for the resistivity of polycrystalline Fe_3O_4 produced by laser ablation.[45] The temperature dependence of the in-plane resistivity suggests that electrical transport in electrodeposited films of Fe_3O_4 is controlled by tunneling of electrons between the columnar Fe_3O_4 grains through insulating γ–Fe_2O_3 grain boundaries. For a typical probe spacing of

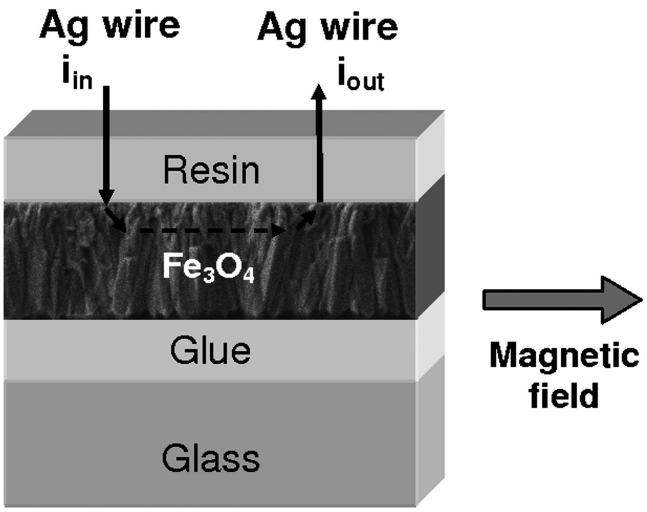

FIG. 7. Schematic illustration of the sample configuration for the electrical transport and magnetoresistance measurements.

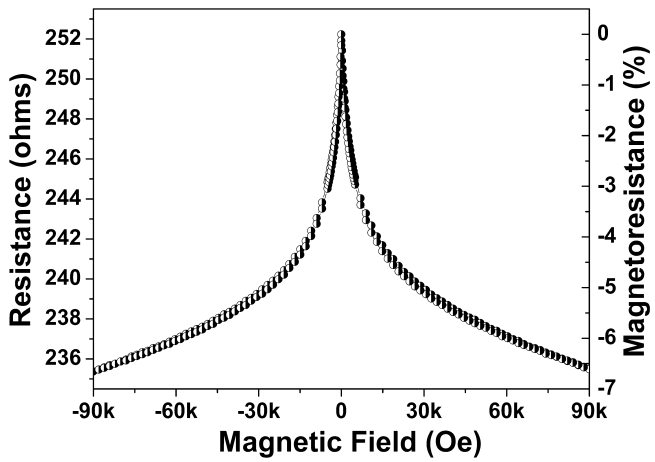

FIG. 9. Effect of magnetic field on the in-plane resistance of the electrodeposited Fe_3O_4 film. A magnetoresistance of –6.5% was observed at an applied field of 9 T.

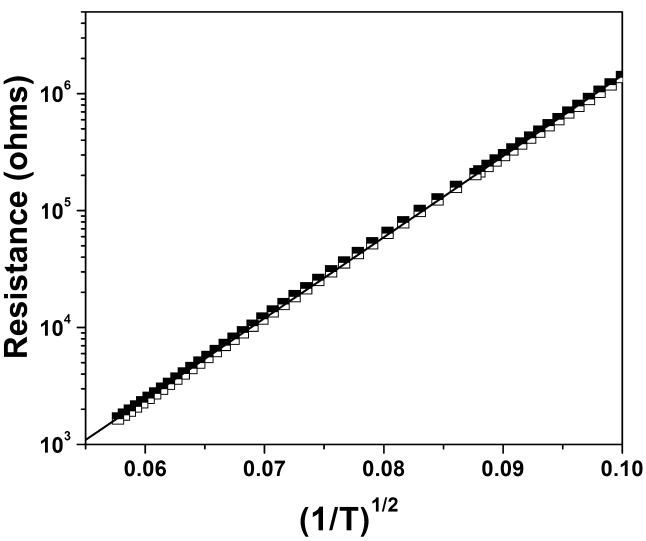

FIG. 8. Effect of temperature on the in-plane resistance of the electrodeposited Fe_3O_4 film. The linear fit of log(R) versus $T^{-1/2}$ is consistent with tunneling across resistive grain boundaries.

5 mm, the current must pass through about 10^4 columnar grains.

Figure 9 shows a plot of the in-plane resistance of a 3-μm-thick film of electrodeposited Fe_3O_4 at room temperature as a function of magnetic field. The magnetic field is aligned parallel with the film in this measurement. The resistance of the film decreases as the applied magnetic field is increased. The resistance does not saturate even at an applied field of 9 T. The magnetoresistance was calculated using Eq. (4).

$$\Delta R = (R_o - R_H)/R_o \quad . \tag{4}$$

A magnetoresistance of –6.5% was observed at 300 K at an applied magnetic field of 9 T. Although not shown here, a commercially purchased Fe_3O_4(111) single crystal exhibited no measurable magnetoresistance. The magnetoresistance behavior is consistent with the model developed by Eerenstein et al., in which spin polarized electrons tunnel across antiphase boundaries.[10,46] We assume in our case that the tunneling of spin polarized electrons occurs across resistive γ–Fe_2O_3 at the columnar grain boundaries. This mechanism has also been proposed by Liu et al. for Fe_3O_4 films grown by reactive sputtering,[45] Serrate et al. for cold pressed nanopowders,[8] and Kitamoto et al. for electrodeposited Fe_3O_4 films.[9] More work needs to be done to determine the exact magnetoresistance mechanism in our electrodeposited films, and to determine whether this magnetoresistance can be tuned by controlling the degree of oxidation of the columnar grain boundaries.

IV. CONCLUSIONS

Films of Fe_3O_4 were electrodeposited by reduction of an Fe(III)-TEA complex in alkaline solution. An electrochemical/chemical mechanism is proposed, in which electrochemically produced Fe^{2+} reacts chemically with Fe(III)-TEA in solution to produce Fe_3O_4. The films deposit with a [100] preferred orientation and a columnar morphology. The columnar nature of the films accentuates the effect of grain boundaries in electrical transport and magnetoresistance measurements. The in-plane resistance of the films can be tuned by controlling the ambient oxygen partial pressure. Exposing the film to O_2 leads to an increase in the in-plane resistance, consistent with oxidation of the grain boundaries to γ–Fe_2O_3. In-plane magnetoresistance values of up to –6.5% at 300 K were observed at an applied magnetic field of 9 T. Although more work needs to be done to determine the magnetoresistance mechanism in the films, we assume

that the process involves tunneling of spin polarized electrons across resistive γ–Fe_2O_3 grain boundaries.

ACKNOWLEDGMENTS

This work was supported by National Science Foundation Grant Nos. CHE-0243424, CHE-0437346, and DMR-0504715, and Department of Energy Grant No. DE-FC07-03ID14509.

REFERENCES

1. Z. Zhang and S. Satpathy: Electron-states, magnetism, and the Verwey transition in magnetite. *Phys. Rev. B* **44,** 13319 (1991).
2. V.I. Anisimov, I.S. Elfimov, N. Hamada, and K. Terakura: Charge-ordered insulating state of Fe_3O_4 from first-principles electronic-structure calculations. *Phys. Rev. B* **54,** 4387 (1996).
3. Y.S. Dedkov, U. Rudiger, and G. Guntherodt: Evidence for the half-metallic ferromagnetic state of Fe_3O_4 by spin-resolved photoelectron spectroscopy. *Phys. Rev. B* **65,** 064417 (2002).
4. T.A. Sorenson, S.A. Morton, D.G. Waddill, and J.A. Switzer: Epitaxial electrodeposition of Fe_3O_4 thin films on the low-index planes of gold. *J. Am. Chem. Soc.* **124,** 7604 (2002).
5. G. Hu and Y. Suzuki: Negative spin polarization of Fe_3O_4 in magnetite/manganite-based junctions. *Phys. Rev. Lett.* **89,** 276601 (2002).
6. X.W. Li, A. Gupta, G. Xiao, W. Qian, and V.P. Dravid: Fabrication and properties of heterojunction magnetite (Fe_3O_4) tunnel junctions. *Appl. Phys. Lett.* **73,** 3282 (1998).
7. J.M.D. Coey, A.E. Berkowitz, L. Balcells, F.F. Putris, and F.T. Parker: Magnetoresistance of magnetite. *Appl. Phys. Lett.* **72,** 734 (1998).
8. D. Serrate, J.M. De Teresa, P.A. Algarabel, R. Fernandez-Pacheco, J. Galibert, and M.R. Ibarra: Grain-boundary magnetoresistance up to 42 T in cold-pressed Fe_3O_4 nanopowders. *J. Appl. Phys.* **97,** 084317 (2005).
9. Y. Kitamoto, Y. Nakayama, and M. Abe: Spin-dependent intergranular transport in magnetite films deposited by ferrite plating. *J. Appl. Phys.* **87,** 7130 (2000).
10. W. Eerenstein, T.T.M. Palstra, S.S. Saxena, and T. Hibma: Spin-polarized transport across sharp antiferromagnetic boundaries. *Phys. Rev. Lett.* **88,** 247204 (2002).
11. J.J. Versluijs, M.A. Bari, and J.M.D. Coey: Magnetoresistance of half-metallic oxide nanocontacts. *Phys. Rev. Lett.* **87,** 026601 (2001).
12. G.Q. Gong, A. Gupta, G. Xiao, W. Qian, and V.P. Dravid: Magnetoresistance and magnetic properties of epitaxial magnetite thin films. *Phys. Rev. B* **56,** 5096 (1997).
13. X.W. Li, A. Gupta, G. Xiao, and G.Q. Gong: Transport and magnetic properties of epitaxial and polycrystalline magnetite thin films. *J. Appl. Phys.* **83,** 7049 (1998).
14. S.B. Ogale, K. Ghosh, R.P. Sharma, R.L. Greene, R. Ramesh, and T. Venkatesan: Magnetotransport anisotropy effects in epitaxial magnetite (Fe_3O_4) thin films. *Phys. Rev. B* **57,** 7823 (1998).
15. J. Tang, K-Y. Wang, and W. Zhou: Magnetic properties of nanocrystalline Fe_3O_4 films. *J. Appl. Phys.* **89,** 7690 (2001).
16. J.F. Anderson, M. Kuhn, U. Diebold, K. Shaw, P. Stoyanov, and D. Lind: Surface structure and morphology of Mg-segregated epitaxial Fe_3O_4(001) thin films on MgO(001). *Phys. Rev. B* **56,** 9902 (1997).
17. K.A. Shaw, E. Lochner, and D.M. Lind: Interdiffusion study of magnesium in magnetite thin films grown on magnesium oxide (001) substrates. *J. Appl. Phys.* **87,** 1727 (2000).
18. R.F.C. Farrow, P.M. Rice, M.F. Toney, R.F. Marks, J.A. Hendstrom, R. Stephenson, M.J. Carey, and A.J. Kellock: Nanoscale phase separation in Fe_3O_4(111) films on sapphire(0001) and phase stability of Fe_3O_4(001) films on MgO(001) grown by oxygen-plasma-assisted molecular-beam epitaxy. *J. Appl. Phys.* **93,** 5626 (2003).
19. W. Weiss and M. Ritter: Metal oxide heteroepitaxy: Stranski-Krastanov growth for iron oxides on Pt(111). *Phys. Rev. B* **59,** 5201 (1999).
20. R.L. Kurtz, J. Karunamuni, and R.L. Stockbauer: Synthesis of epitaxial Fe_3O_4 films on Cu(001). *Phys. Rev. B* **60,** 16342 (1999).
21. J.A. Switzer, M.G. Shumsky, and E.W. Bohannan: Electrodeposited ceramic single crystals. *Science* **284,** 293 (1999).
22. E.W. Bohannan, M.G. Shumsky, and J.A. Switzer: Epitaxial electrodeposition of copper(I) oxide on single-crystal gold(100). *Chem. Mater.* **11,** 2289 (1999).
23. M.P. Nikiforov, A.A. Vertegel, M.G. Shumsky, and J.A. Switzer: Epitaxial electrodeposition of Fe_3O_4 on single-crystal Au(111). *Adv. Mater.* **12,** 1351 (2000).
24. R. Liu, A.A. Vertegel, E.W. Bohannan, T.A. Sorenson, and J.A. Switzer: Epitaxial electrodeposition of zinc oxide nanopillars on single-crystal gold. *Chem. Mater.* **13,** 508 (2001).
25. J.A. Switzer, H.M. Kothari, and E.W. Bohannan: Thermodynamic to kinetic transition in epitaxial electrodeposition. *J. Phys. Chem. B* **106,** 4027 (2002).
26. H.M. Kothari, A.A. Vertegel, E.W. Bohannan, and J.A. Switzer: Epitaxial electrodeposition of Pb–Tl–O superlattices on single-crystal Au(100). *Chem. Mater.* **14,** 2750 (2002).
27. R. Liu, E.W. Bohannan, J.A. Switzer, F. Oba, and F. Ernst: Epitaxial electrodeposition of Cu_2O films onto InP(001). *Appl. Phys. Lett.* **83,** 1944 (2003).
28. S. Nakanishi, G.T. Lu, H.M. Kothari, E.W. Bohannan, and J.A. Switzer: Epitaxial electrodeposition of Prussian Blue thin films on single-crystal Au(110). *J. Am. Chem. Soc.* **125,** 14998 (2003).
29. R. Liu, F. Oba, E.W. Bohannan, F. Ernst, and J.A. Switzer: Shape control in epitaxial electrodeposition: Cu_2O nanocubes on InP(001). *Chem. Mater.* **15,** 4882 (2003).
30. J.A. Switzer, H.M. Kothari, P. Poizot, S. Nakanishi, and E.W. Bohannan: Enantiospecific electrodeposition of a chiral catalyst. *Nature* **425,** 490 (2003).
31. E.W. Bohannan, H.M. Kothari, I.M. Nicic, and J.A. Switzer: Enantiospecific electrodeposition of chiral CuO films on single-crystal Cu(111). *J. Am. Chem. Soc.* **126,** 488 (2004).
32. R. Liu, E.A. Kulp, F. Oba, E.W. Bohannan, F. Ernst, and J.A. Switzer: Epitaxial electrodeposition of high-aspect-ratio Cu_2O(110) nanostructures on InP(111). *Chem. Mater.* **17,** 725 (2005).
33. F. Oba, F. Ernst, Y. Yu, R. Liu, H.M. Kothari, and J.A. Switzer: Epitaxial growth of cuprous oxide electrodeposited onto semiconductor and metal substrates. *J. Am. Ceram. Soc.* **88,** 253 (2005).
34. M. Abe: Ferrite plating: A chemical method preparing oxide magnetic films at 24–100 °C, and its applications. *Electrochim. Acta* **45,** 3337 (2000).
35. M. Abe and Y. Tamura: Ferrite-plating in aqueous solution: A new method for preparing magnetic thin film. *Jpn. J. Appl. Phys.* **22,** L511 (1983).
36. D. Carlier, C. Terrier, C. Arm, and J-Ph. Ansermet: Preparation and magnetic properties of Fe_3O_4 nanostructures grown by electrodeposition. *Electrochem. Solid State Lett.* **8,** C43 (2005).
37. R.S. Sapieszko and E. Matijevic: Preparation of well-defined colloidal particles by thermal decomposition of metal chelates. I. Iron oxides. *J. Colloid Interface Sci.* **74,** 405 (1980).
38. C. Ruby, C. Humbert, and J. Fusy: Surface and interface properties of epitaxial iron oxide thin films deposited on MgO(001)

studied by XPS and Raman spectroscopy. *Surf. Interface Anal.* **29,** 377 (2000).

39. S.A. Krasnikov, A.S. Vinogradov, K-H. Hallmeier, R. Höhne, M. Ziese, P. Esquinazi, T. Chassé, and R. Szargan: Oxidation effects in epitaxial Fe_3O_4 layers on MgO and $MgAl_2O_4$ substrates studied by x-ray absorption, fluorescence, and photoemission. *Mater. Sci. Eng. B* **109,** 207 (2004).
40. J.P. Saunders and P.K. Gallagher: Thermomagnetometric evidence of γ–Fe_2O_3 as an intermediate in the oxidation of magnetite. *Thermochim. Acta* **406,** 241 (2003).
41. K.J. Gallagher, W. Feitknecht, and U. Mannweler: Mechanism of oxidation of magnetite to γ–Fe_2O_3. *Nature* **217,** 1118 (1968).
42. P.S. Sidhu, R.J. Gilkes, and A.M. Posner: Mechanism of the low temperature oxidation of synthetic magnetites. *J. Inorg. Nucl. Chem.* **39,** 1953 (1977).
43. J. Tang, M. Myers, K.A. Bosnick, and L.E. Brus: Magnetite Fe_3O_4 nanocrystals: spectroscopic observation of aqueous oxidation kinetics. *J. Phys. Chem. B* **107,** 7501 (2003).
44. P. Sheng, B. Abeles, and Y. Arie: Hopping conductivity in granular metals. *Phys. Rev. Lett.* **31,** 44 (1973).
45. H. Liu, E.Y. Jiang, H.L. Bai, R.K. Zheng, H.L. Wei, and X.X. Zhang: Large room-temperature spin-dependent tunneling magnetoresistance in polycrystalline Fe_3O_4 films. *Appl. Phys. Lett.* **83,** 3531 (2003).
46. W. Eerenstein, T.T.M. Palstra, T. Hibma, and S. Celotto: Origin of the increased resistivity in epitaxial Fe_3O_4 films. *Phys. Rev. B* **66,** 201101 (R) (2002).